ACS Photonics

pubs.acs.org/journal/apchd5

Article

Nonlinear Excitation and Self-Action of Bloch Surface Waves Governed by Gradient Optical Forces

Daniil A. Shilkin, Evgeny V. Lyubin, and Andrey A. Fedyanin*

Cite This: *ACS Photonics* 2022, 9, 211−216

Read Online

ACCESS | Metrics & More | Article Recommendations | Supporting Information

ABSTRACT: Self-action of light is among the most important nonlinear optical effects with a plethora of present and potential applications. Suspensions of subwavelength particles are characterized by high artificial optical nonlinearity induced by gradient optical forces. Here, we report on an experimental study of self-action of the Bloch surface wave (BSW) excited at the interface between a one-dimensional photonic crystal and a water suspension of dielectric nanoparticles by a continuous-wave diode laser. We demonstrate the modification of the BSW resonance with increasing optical power and, for the first time to our knowledge, experimentally show self-focusing of BSWs. A plane-wave model is used to describe the mechanism of the observed resonance modification. Our results demonstrate the great potential of guided waves in multilayer structures for optical signal processing and open up new possibilities for the light-controlled operation of BSWs.

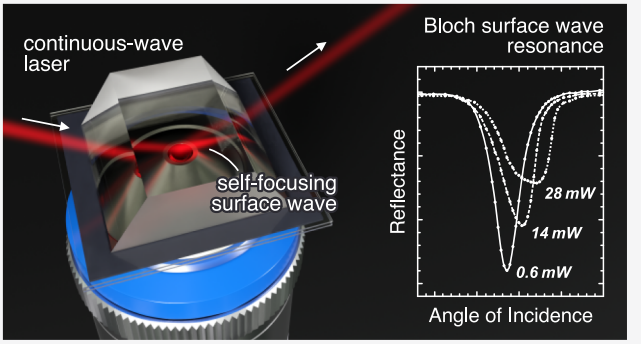

KEYWORDS: *nonlinear optics, soft matter, photonic crystals, optical forces, Bloch surface waves, self-focusing*

Nonlinear optics and self-action of light have been fascinating scientists for more than half a century.[1] A rich variety of nontrivial phenomena occurring when light propagates through a nonlinear medium have been of ongoing interest due to their numerous applications in research and industry.[2−4] Many of these phenomena are the result of the refractive index being dependent on the intensity of light. In most materials, this dependence becomes significant only at high power levels, typically requiring high-energy pulsed laser sources. This, however, is not the case when composite materials are used.

Soon after Ashkin first observed gradient optical forces,[5] aerosol and liquid suspensions of small particles were shown to exhibit strong artificial nonlinearities.[6,7] When particles in such media are subject to a laser beam, they tend to be localized in the intensity maxima. As a result, the particle concentration and the effective refractive index increase in regions of high light intensity. This behavior is analogous to that of a homogeneous Kerr medium and allows for the observation of the same nonlinear effects, such as degenerate four-wave mixing, self-focusing, and self-trapping of light.[8,9] Suspensions, however, are characterized by much higher nonlinear coefficients coming at the cost of slower response.

Over the past few decades, a variety of studies using liquid suspensions as nonlinear optical media have been reported. The interface between a dielectric crystal and a suspension of quartz nanoparticles has been shown to exhibit optical switching behavior.[10] Modulation instability and optical spatial soliton arrays have been observed in suspensions of subwavelength dielectric particles in the presence of unpatterned evanescent waves.[11] A number of papers have been devoted to self-guiding and enhanced transmission of light in different kinds of liquid suspensions.[12−14] Being placed in two counterpropagating laser beams, dielectric suspensions have been shown to act as an optically tunable gradient index lens.[15] Recently, modulation instability of optical vortex beams in a negative polarizability suspension has been observed.[16] While the direct applications of the discussed phenomena are currently being explored, liquid suspensions have already been established as a powerful tool for model experiments.

Bloch surface waves (BSWs) are propagating surface modes in photonic crystals. They have mainly been studied in one-dimensional photonic crystals composed of periodic dielectric multilayers.[17] Similar to surface plasmon waves in metal films, BSWs are confined to the surface and can be resonantly excited by prism coupling.[18] In contrast to surface plasmons, BSWs are typically characterized by much higher quality factors and negligible thermal losses.[19] Moreover, the dispersion of BSWs can be easily tuned by varying the thicknesses of the layers forming the photonic crystal structure.[20] Due to these

Received: September 13, 2021
Published: January 7, 2022

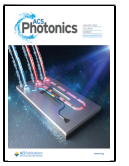

https://doi.org/10.1021/acsphotonics.1c01402
ACS Photonics 2022, 9, 211−216

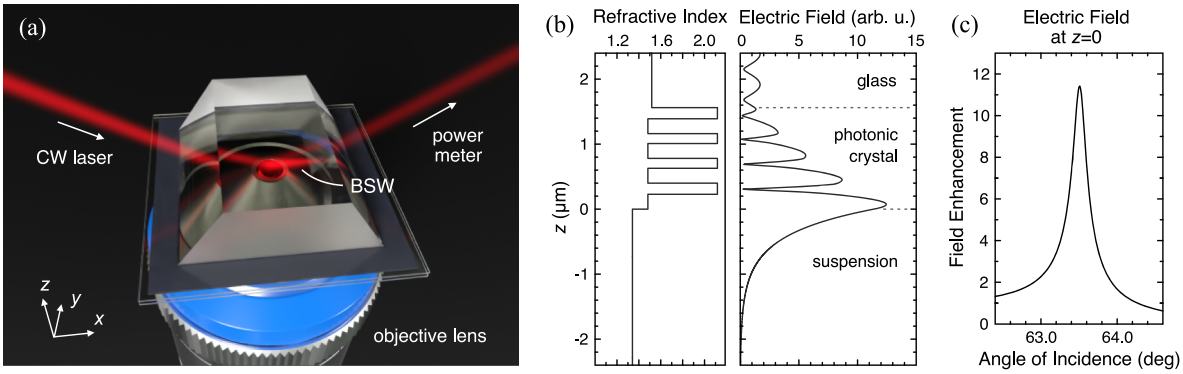

Figure 1. (a) Experimental schematic. CW, continuous wave; BSW, Bloch surface wave. (b) Structure of the studied sample and electric field amplitude profile at the BSW resonance calculated for low-power plane-wave excitation at 638 nm. (c) Electric field enhancement at the photonic crystal surface as a function of the angle of incidence in the glass substrate.

properties, BSWs have been repeatedly used for sensing[21,22] optical trapping, and manipulation[23,24] and have been suggested as an alternative platform for two-dimensional integrated optics.[25−28] Finally, BSWs are potentially useful for optical signal processing and have recently been exploited to demonstrate all-optical switching.[29] Although some studies have used BSWs to enhance nonlinear optical effects,[30,31] the self-action of BSWs, to the best of our knowledge, has never been considered.

In this Article, we report on an experiment that reveals nonlinear processes accompanying the excitation and propagation of BSWs in the presence of Kerr optical nonlinearity. We study self-action of the BSW at the interface between a one-dimensional photonic crystal and a water suspension of dielectric nanoparticles. We demonstrate the modification of the BSW resonance with increasing optical power and experimentally show self-focusing of the BSW.

The experimental arrangement is illustrated in Figure 1a. The BSW is excited in the Kretschmann prism configuration using a single-mode continuous-wave diode laser operating at 638 nm. The excitation beam is *s*-polarized and incident on the photonic crystal surface at a variable angle; the beam is slightly focused on the surface with a controlled angle divergence. The excitation of the BSW is experimentally revealed by measuring the angular reflectance spectrum and visualized using optical scattering microscopy; see Methods for more details of the experimental setup.

The photonic crystal structure under study is shown in the left panel of Figure 1b. It consists of four pairs of Ta_2O_5 and SiO_2 quarter-wavelength layers deposited on a Schott D263T glass substrate by magnetron sputtering; the band gap central wavelength at normal incidence is 1.3 μm. The sample was experimentally characterized by spectroscopic ellipsometry to specify the thicknesses of individual layers; see Methods for details of the characterization procedure. The obtained values were used in further calculations. As a nonlinear medium, we used a water suspension of 47 nm polystyrene particles with a concentration of 25 mg/mL. The effective refractive index of the suspension was calculated using the Maxwell-Garnett approximation[32] and, in the absence of powerful light, was found to be 1.337. The suspension refractive index was also assigned a constant imaginary part of 5×10^{-4}, which does not significantly change the calculated field values, but provides a dip in the reflectance spectrum with a product of the width and the depth close to the experimental one. Note that the primary source of the loss modeled using the introduced coefficient is scattering, while the actual absorption of light at 638 nm is relatively negligible.[33,34]

To study the light propagation in the system theoretically, we employed the transfer matrix technique. At low powers, the suspension acts as a linear medium: the particles do not significantly change their spatial distribution in response to the BSW excitation, and the effective refractive index can be considered constant. The BSW field profile calculated for this case is shown in the right panel of Figure 1b. It was obtained assuming a plane wave with the wavelength of 638 nm incident on the photonic crystal surface from the side of the glass at a resonant angle of 63.5°. The angular dependence of the electric field amplitude at the surface is shown in Figure 1c. In the resonance, it is enhanced more than 11 times compared to the incident wave field.

When a high optical power is used, the particles change their spatial distribution under the action of optical forces; in the relevant case of small particles, the gradient optical forces dominate the scattering ones.[35] As a result, the particles tend to be localized in the BSW excitation region and, consequently, they modify the BSW resonance with increasing optical power. Note that the particles are not stably trapped in the BSW evanescent field; however, while they are undergoing Brownian motion, their average concentration is governed by the intensity profile. We have modeled the occurring processes using an approach similar to that used elsewhere.[36] The suspension was considered as a stack of 50 uniform layers with the refractive index n, depending linearly on the intensity of light:

$$n(I) = n_0 + n_2 I \tag{1}$$

The optical Kerr coefficient $n_2 = 6.2 \times 10^{-14}$ m^2 W^{-1} was found using the Taylor expansion for particle concentration, which was assumed to follow the Boltzmann distribution. We also assumed that, in equilibrium, the refractive index of the suspension decreases exponentially with the distance from the surface:

$$n(z) = n_0 + n_{\text{plus}} e^{-|z|/d} \tag{2}$$

where d is equal to the penetration depth of optical power at low intensities and n_{plus} is the light-induced increment of the refractive index of the suspension near the surface. By using the transfer matrix technique, for each angle of incidence, we calculated the field enhancement L at the photonic crystal

https://doi.org/10.1021/acsphotonics.1c01402
ACS Photonics 2022, 9, 211−216

surface as a function of the parameter n_{plus}. Considering eqs 1 and 2 at $z = 0$, we obtain the following transcendent equation:

$$n_{plus} = n_2 L^2(n_{plus}) I_0 \quad (3)$$

it was then solved numerically for n_{plus} as a function of the incident light intensity I_0. Finally, the reflectance was found for the determined n_{plus} values using the transfer matrix technique. The whole procedure was repeated independently for every considered angle of incidence.

The resulting reflectance spectra calculated for the indicated intensities of the incident light are shown in Figure 2a; the inset shows the angular dependences of the field enhancement L. In the linear case, when the intensity is low and the refractive index of the suspension is constant, the BSW resonance dip in the reflectance spectrum has a symmetric shape similar to that of the field-enhancement peak. With increasing intensity, the resonant angle of incidence shifts to the higher values and the curve shape is significantly modified. To better understand this behavior, let us consider the case of a fixed angle of incidence. For example, if it is set to provide resonant excitation at low power, as the power increases, the effective refractive index in the BSW evanescent field increases, resulting in less-efficient BSW excitation. On the other hand, if the angle of incidence is detuned from the resonance value to a higher one, then as the optical power increases, the resonance shifts to the set value, and the excitation becomes more efficient. In contrast to the case of an externally pumped system,[37] here, the resonance does not retain its shape upon displacement since the modifications substantially depend on the resonant amplification of the incident light. Note that for some angles of incidence, the model predicts bistable behavior, which means that two stable particle distributions can be obtained depending on the previous configuration. For example, at an angle of incidence of 63.9° and an intensity of 300 kW/cm^2, the reflectance can be either 0.31 or 0.98. In the first case, the particles are strongly concentrated near the surface, and the BSW is resonantly excited, as evidenced by the field enhancement reaching the value of 12.7. In the second case, the particles are distributed more uniformly, and the BSW is not excited.

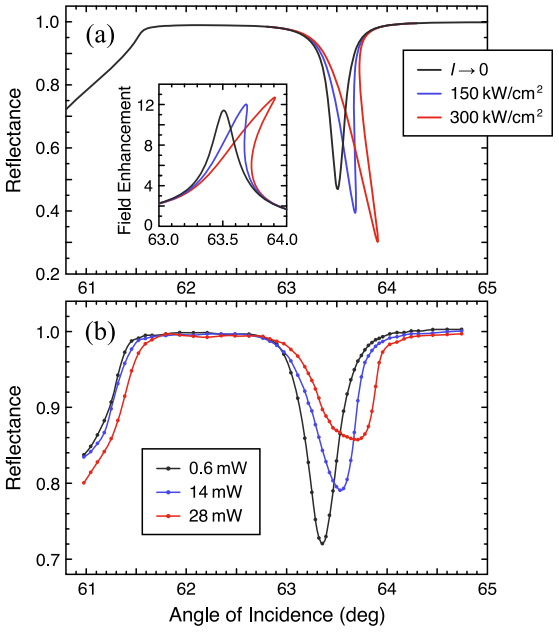

Figure 2. Nonlinear modification of the BSW resonance. (a) Angular reflectance spectra calculated in the plane wave approximation for different incident light intensities. The inset shows the corresponding field enhancement dependences. (b) Experimental angular reflectance spectra for different powers of the incident beam. The angle of incidence is measured inside the glass substrate.

In the experiment, we also observe modification of the BSW resonance. The measured angular reflectance spectra for three values of incident power are demonstrated in Figure 2b. Here we plot the equilibrium reflectance values that were reached within a few seconds after setting the angle of incidence. The critical angle of total reflection is visible on the left part of the plot. It is found to be about 61.4° and slightly rising with increasing optical power due to the change of the refractive index in the vicinity of the surface.[10] The BSW resonance modifies more significantly. At a power of 0.6 mW, it reveals itself as a symmetric dip centered at 63.35° with the width determined by the angular divergence of the incident beam; the corresponding effective refractive index of the BSW mode is 1.359. With increasing optical power, the dip shape is modified and the resonance position shifts by more than 0.3°, which corresponds to the effective refractive index change of 0.004. This observation is, in general, in agreement with our theoretical results. However, experimentally, we observe a decrease in the depth of the dip, while theoretically it was predicted to increase. Moreover, experimentally we do not observe the expected bistability. This can be associated with the use of the plane-wave approximation in our calculations, while the role of transverse intensity gradients in the studied processes may be crucial. First, when a Gaussian beam is used, some angular components may fulfill the resonant conditions, even at a nonresonant angle of incidence. Second, when the particles are redistributed in the direction perpendicular to the surface, their distribution along the surface also changes. This, in turn, leads to the enhanced scattering loss in regions of high intensity and can be a reason for the observed decrease in the resonance quality factor. Note that bistability may still be present in this system at higher intensities. However, the range of the used optical power in our measurements was limited by the adhesion of particles to the photonic crystal surface: at the power values exceeding 30 mW, the stabilization time increased significantly and the modifications became irreversible.

The observed modification of the surface wave resonance highlights the potential of BSWs for optical processing applications. An important challenge on the way to all-optical signal processing is the development of efficient optical switches for modulating light with light.[38,39] Due to the high quality factor and sensitivity of the surface wave resonance to the local surface properties, BSW excitation can be controlled using low operating powers. With a proper choice of nonlinear materials, BSWs can be exploited to create low-power all-optical switches. Being intrinsically planar, these devices would be suitable for direct integration into compact photonic circuits. For example, the recently demonstrated Mach–Zehnder interferometer for BSWs[27] may operate as an optical switch if a nonlinear material is introduced to one of the arms.

The slow response of the involved nonlinearity makes it possible to visualize the temporal evolution of the BSW excitation by means of conventional optical microscopy. Figure 3a shows a time-sequenced set of microimages obtained at an incident power of 50 mW and an angle of incidence exceeding

https://doi.org/10.1021/acsphotonics.1c01402
ACS Photonics 2022, 9, 211−216

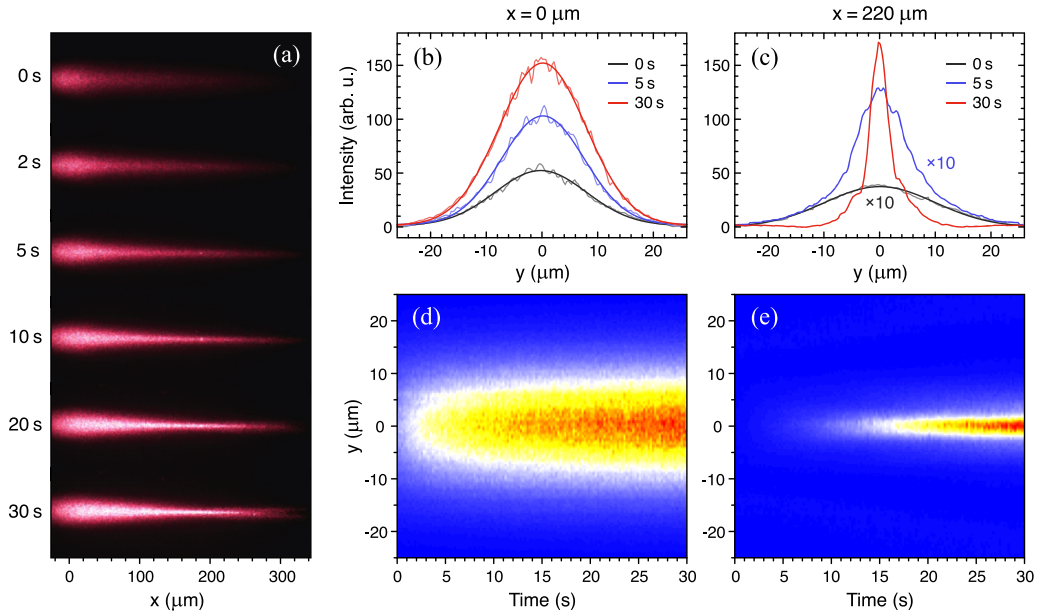

Figure 3. Self-focusing of the BSW. (a) Set of microimages showing the temporal evolution of the BSW intensity distribution in the $x-y$ plane. (b–e) Transverse intensity distribution (b, d) at the position of the excitation beam waist and (c, e) 220 μm away from that. Bright curves in (b) and the black one in (c) show Gaussian fits to the corresponding experimental data.

the resonant value by approximately 0.5°. The original video is available in the Supporting Information. Due to light scattering by suspended particles, the intensity distribution in the vicinity of the surface is naturally observed. We should note, however, that the registered intensity is not directly proportional to the BSW intensity profile since it also depends on the concentration of scattering particles. At the initial moment, the laser turns on. The waist of the incident beam is clearly visible in the left part of the image, while the comet-shaped BSW tail is less pronounced, which is characteristic for excitation at a slightly off-resonance angle of incidence.[40] As time goes by and the particles rearrange, the observed intensity distribution is significantly modified. The temporal evolution of transverse intensity profiles is shown in Figure 3b–e; see Methods for the description of the video processing. In the vicinity of the excitation beam waist (x = 0 μm; see Figure 3b,d), the profile at any time is well approximated by a Gaussian curve with a full width at half-maximum of 19 μm varying within 10%. The absolute intensity increases with time, which is explained by the shift of the BSW resonance toward the actual angle of incidence and more efficient excitation of the BSW. Meanwhile, the BSW tail becomes not only brighter but also much narrower. Its intensity profile at a distance of 220 μm from the waist is shown in Figure 3c,e. After a few seconds, the observed distribution ceases to be Gaussian, and its width shrinks down to 4 μm at half-maximum. We attribute this behavior to the well-known self-focusing effect arising as the consequence of a nonuniform refractive index increase;[41] further changes in the registered light distribution may be explained by the slow adhesion of particles to the photonic crystal surface. The effective refractive index change needed to obtain the self-focusing effect in our experiment can be estimated as follows:[1]

$$\frac{\Delta n_{\mathrm{eff}}}{n_{\mathrm{eff}}} \gtrsim \frac{\lambda^2}{n_{\mathrm{eff}}^2 w_0^2}$$

Here, n_{eff} = 1.359 is the effective refractive index of the BSW mode, w_0 = 16 μm is the excitation beam radius, and λ = 638 nm is the vacuum wavelength. According to our estimation, self-focusing overcomes diffraction at $\Delta n_{\mathrm{eff}} \gtrsim 10^{-3}$ that corresponds to the incident power in the order of units of milliwatts. Note that the use of a wider excitation beam would further decrease the threshold; however, the resulting focal distance would be increased.[1]

Being well studied for bulk light,[1] self-focusing has only recently been experimentally demonstrated for surface plasmon polaritons[42] and, to the best of our knowledge, has never been shown for BSWs. Meanwhile, this phenomenon may find numerous applications in two-dimensional integrated optics and functionalized microfluidic systems. By now, focused BSWs have been formed either by excitation with ring-shaped laser beams[24,43] or by using prefabricated two-dimensional focusing structures.[44−47] Kerr nonlinearity and self-focusing effect expand this toolbox and open new opportunities for the light-controlled operation of BSWs. In perspective, this effect can be used to design integrated adjustable lenses and passive mode lockers on the BSW platform.

In summary, we have demonstrated the excitation and propagation of the Bloch surface wave at the interface between a dielectric multilayer and a nonlinear Kerr medium. The use of a liquid suspension of dielectric nanoparticles as the nonlinear medium has allowed us to observe nontrivial self-action processes with a continuous-wave excitation of moderate power. We anticipate that our results will stimulate further research on optical switching and self-action of BSWs with potential applications in optical manipulation, sensing, and signal processing.

METHODS

Experimental Setup. The BSW excitation was realized in the Kretschmann configuration using a prism with an angle of 54.6° and a refractive index of 1.66. The optical contact between the prism and the glass substrate was maintained by

https://doi.org/10.1021/acsphotonics.1c01402
ACS Photonics 2022, 9, 211−216

immersion oil. The suspension was contained in a chamber made of the photonic crystal sample, a cover glass, and a piece of 0.2 mm thick adhesive tape with a hole. The reflectance spectra were measured using a photodiode-based laser power meter. For each angle of incidence, the reflectance was recorded when the registered power varied within 0.2% for 10 s. The microscopy visualization was performed using a dry objective lens with a numerical aperture of 0.85; the objective field of view was imaged on a CMOS camera (Thorlabs DCC1645C) using a system of achromatic doublets providing a total magnification of 12.5×. During the reflectance measurements, the half angle divergence of the excitation beam in glass was 0.2°, and to demonstrate self-focusing, it was increased to approximately 0.5°.

Sample Characterization. The photonic crystal sample was characterized using a Sentech SE800 ellipsometer. The measurements were performed at angles of incidence of 75° and 80°. In order to get the starting values of the layer thicknesses for the model, a cleaved edge of the sample was visualized by scanning electron microscopy. From ellipsometry, the following values were obtained. The thicknesses of Ta_2O_5 layers, starting from the side of the substrate: 156.3, 160.1, 159.1, and 160.4 nm; the thicknesses of SiO_2 layers: 230.5, 227.6, 228.4, and 235.1 nm. The refractive indices of Ta_2O_5 and SiO_2 layers at 638 nm are, respectively, 2.135 and 1.478; that of the glass substrate is 1.521. These values were used in the calculations.

Video Processing. The microscopic video was captured at the frame rate of 17.52 s^{-1} and analyzed using ImageJ software. In order to get data in a broad dynamic range and avoid off-scale artifacts, the red and green channels have been processed independently. The red channel was found to be the most sensitive to the laser radiation at 638 nm; it was used to get the profiles shown in Figure 3c by the black and blue curves. The signal in the green channel was found to correlate with the signal in the red one with a linear coefficient of 0.13; the green channel was used to get the rest of the profiles. The data processing consisted in subtracting the dark noise and averaging over 4 frames that corresponds to the total exposure time of 0.23 s and over 70 pixels along x-direction that corresponds to 20 μm on the sample. The profiles extracted from the red channel were additionally multiplied by the specified coefficient so that they could be compared with the other results.

■ ASSOCIATED CONTENT

Supporting Information

The Supporting Information is available free of charge at https://pubs.acs.org/doi/10.1021/acsphotonics.1c01402.

Microscopic video of self-focusing of the Bloch surface wave (MOV)

■ AUTHOR INFORMATION

Corresponding Author

Andrey A. Fedyanin − *Faculty of Physics, Lomonosov Moscow State University, Moscow 119991, Russia;* orcid.org/0000-0003-4708-6895; Email: fedyanin@nanolab.phys.msu.ru

Authors

Daniil A. Shilkin − *Faculty of Physics, Lomonosov Moscow State University, Moscow 119991, Russia;* orcid.org/0000-0001-7597-2734

Evgeny V. Lyubin − *Faculty of Physics, Lomonosov Moscow State University, Moscow 119991, Russia*

Complete contact information is available at: https://pubs.acs.org/10.1021/acsphotonics.1c01402

Notes

The authors declare no competing financial interest.

■ ACKNOWLEDGMENTS

The authors acknowledge ellipsometry measurements by Alexander Ezhov and Alla Chebotareva, scanning electron microscopy by Vladislav Sitnianskii, and valuable comments from Matvey Pochechuev, Kirill Safronov, and Anna Popkova. This work was partially supported by the Russian Science Foundation (#21-72-00123). D.A.S. and E.V.L. acknowledge support from the MSU Quantum Technology Centre. A.A.F. acknowledges the Interdisciplinary Scientific and Educational School of the Lomonosov Moscow State University "Photonic and Quantum Technologies. Digital Medicine".

■ REFERENCES

(1) Shen, Y.-R. *The Principles of Nonlinear Optics*; Wiley-Interscience: New York, 1984.

(2) Keller, U. Recent developments in compact ultrafast lasers. *Nature* **2003**, *424*, 831−838.

(3) Kasparian, J.; Rodriguez, M.; Méjean, G.; Yu, J.; Salmon, E.; Wille, H.; Bourayou, R.; Frey, S.; André, Y.-B.; Mysyrowicz, A.; et al. White-light filaments for atmospheric analysis. *Science* **2003**, *301*, 61−64.

(4) Helmchen, F.; Denk, W. Deep tissue two-photon microscopy. *Nat. Methods* **2005**, *2*, 932−940.

(5) Ashkin, A. Acceleration and trapping of particles by radiation pressure. *Phys. Rev. Lett.* **1970**, *24*, 156−159.

(6) Palmer, A. J. Nonlinear optics in aerosols. *Opt. Lett.* **1980**, *5*, 54−55.

(7) Smith, P. W.; Maloney, P. J.; Ashkin, A. Use of a liquid suspension of dielectric spheres as an artificial Kerr medium. *Opt. Lett.* **1982**, *7*, 347−349.

(8) Smith, P. W.; Ashkin, A.; Tomlinson, W. J. Four-wave mixing in an artificial Kerr medium. *Opt. Lett.* **1981**, *6*, 284−286.

(9) Ashkin, A.; Dziedzic, J. M.; Smith, P. W. Continuous-wave self-focusing and self-trapping of light in artificial Kerr media. *Opt. Lett.* **1982**, *7*, 276−278.

(10) Smith, P. W.; Tomlinson, W. J. Nonlinear optical interfaces: Switching behavior. *IEEE J. Quantum Electron.* **1984**, *20*, 30−36.

(11) Reece, P. J.; Wright, E. M.; Dholakia, K. Experimental observation of modulation instability and optical spatial soliton arrays in soft condensed matter. *Phys. Rev. Lett.* **2007**, *98*, 203902.

(12) Man, W.; Fardad, S.; Zhang, Z.; Prakash, J.; Lau, M.; Zhang, P.; Heinrich, M.; Christodoulides, D. N.; Chen, Z. Optical nonlinearities and enhanced light transmission in soft-matter systems with tunable polarizabilities. *Phys. Rev. Lett.* **2013**, *111*, 218302.

(13) Fardad, S.; Salandrino, A.; Heinrich, M.; Zhang, P.; Chen, Z.; Christodoulides, D. N. Plasmonic resonant solitons in metallic nanosuspensions. *Nano Lett.* **2014**, *14*, 2498−2504.

(14) Gautam, R.; Xiang, Y.; Lamstein, J.; Liang, Y.; Bezryadina, A.; Liang, G.; Hansson, T.; Wetzel, B.; Preece, D.; White, A.; et al. Optical force-induced nonlinearity and self-guiding of light in human red blood cell suspensions. *Light Sci. Appl.* **2019**, *8*, 31.

(15) Brzobohatý, O.; Chvátal, L.; Šiler, M.; Zemánek, P. Complex colloidal structures with non-linear optical properties formed in an optical trap. *Opt. Express* **2020**, *28*, 37700−37707.

(16) Sun, J.; Silahli, S. Z.; Walasik, W.; Li, Q.; Johnson, E.; Litchinitser, N. M. Nanoscale orbital angular momentum beam instabilities in engineered nonlinear colloidal media. *Opt. Express* **2018**, *26*, 5118−5125.
(17) Khan, M. U.; Corbett, B. Bloch surface wave structures for high sensitivity detection and compact waveguiding. *Sci. Technol. Adv. Mater.* **2016**, *17*, 398−409.
(18) Robertson, W. M.; May, M. S. Surface electromagnetic wave excitation on one-dimensional photonic band-gap arrays. *Appl. Phys. Lett.* **1999**, *74*, 1800−1802.
(19) Sinibaldi, A.; Danz, N.; Descrovi, E.; Munzert, P.; Schulz, U.; Sonntag, F.; Dominici, L.; Michelotti, F. Direct comparison of the performance of Bloch surface wave and surface plasmon polariton sensors. *Sens. Actuators B Chem.* **2012**, *174*, 292−298.
(20) Yariv, A.; Yeh, P. *Optical Waves in Crystals*; Wiley-Interscience: New York, 1984.
(21) Qiao, H.; Guan, B.; Gooding, J. J.; Reece, P. J. Protease detection using a porous silicon based Bloch surface wave optical biosensor. *Opt. Express* **2010**, *18*, 15174−15182.
(22) Tu, T.; Pang, F.; Zhu, S.; Cheng, J.; Liu, H.; Wen, J.; Wang, T. Excitation of Bloch surface wave on tapered fiber coated with one-dimensional photonic crystal for refractive index sensing. *Opt. Express* **2017**, *25*, 9019−9027.
(23) Shilkin, D. A.; Lyubin, E. V.; Soboleva, I. V.; Fedyanin, A. A. Direct measurements of forces induced by Bloch surface waves in a one-dimensional photonic crystal. *Opt. Lett.* **2015**, *40*, 4883−4886.
(24) Xiang, Y.; Tang, X.; Fu, Y.; Lu, F.; Kuai, Y.; Min, C.; Chen, J.; Wang, P.; Lakowicz, J. R.; Yuan, X.; et al. Trapping metallic particles using focused Bloch surface waves. *Nanoscale* **2020**, *12*, 1688−1696.
(25) Descrovi, E.; Sfez, T.; Quaglio, M.; Brunazzo, D.; Dominici, L.; Michelotti, F.; Herzig, H. P.; Martin, O. J. F.; Giorgis, F. Guided Bloch surface waves on ultrathin polymeric ridges. *Nano Lett.* **2010**, *10*, 2087−2091.
(26) Wang, R.; Chen, J.; Xiang, Y.; Kuai, Y.; Wang, P.; Ming, H.; Lakowicz, J. R.; Zhang, D. Two-dimensional photonic devices based on Bloch surface waves with one-dimensional grooves. *Phys. Rev. Appl.* **2018**, *10*, 024032.
(27) Safronov, K. R.; Gulkin, D. N.; Antropov, I. M.; Abrashitova, K. A.; Bessonov, V. O.; Fedyanin, A. A. Multimode interference of Bloch surface electromagnetic waves. *ACS Nano* **2020**, *14*, 10428−10437.
(28) Gulkin, D. N.; Popkova, A. A.; Afinogenov, B. I.; Shilkin, D. A.; Kuršelis, K.; Chichkov, B. N.; Bessonov, V. O.; Fedyanin, A. A. Mie-driven directional nanocoupler for Bloch surface wave photonic platform. *Nanophotonics* **2021**, *10*, 2939−2947.
(29) Popkova, A. A.; Chezhegov, A. A.; Soboleva, I. V.; Rybin, M. G.; Obraztsova, E. D.; Bessonov, V. O.; Fedyanin, A. A. Ultrafast all-optical switching in the presence of Bloch surface waves. *J. Phys. Conf. Ser.* **2020**, *1461*, 012134.
(30) Konopsky, V. N.; Alieva, E. V.; Alyatkin, S. Y.; Melnikov, A. A.; Chekalin, S. V.; Agranovich, V. M. Phase-matched third-harmonic generation via doubly resonant optical surface modes in 1D photonic crystals. *Light Sci. Appl.* **2016**, *5*, e16168.
(31) Guo, Q.; Ou, Z.; Tang, J.; Zhang, J.; Lu, F.; Wu, K.; Zhang, D.; Zhang, S.; Xu, H. Efficient frequency mixing of guided surface waves by atomically thin nonlinear crystals. *Nano Lett.* **2020**, *20*, 7956−7963.
(32) Niklasson, G. A.; Granqvist, C. G.; Hunderi, O. Effective medium models for the optical properties of inhomogeneous materials. *Appl. Opt.* **1981**, *20*, 26−30.
(33) Kedenburg, S.; Vieweg, M.; Gissibl, T.; Giessen, H. Linear refractive index and absorption measurements of nonlinear optical liquids in the visible and near-infrared spectral region. *Opt. Mater. Express* **2012**, *2*, 1588−1611.
(34) Zhang, X.; Qiu, J.; Li, X.; Zhao, J.; Liu, L. Complex refractive indices measurements of polymers in visible and near-infrared bands. *Appl. Opt.* **2020**, *59*, 2337−2344.
(35) Shilkin, D. A.; Lyubin, E. V.; Soboleva, I. V.; Fedyanin, A. A. Near-field probing of Bloch surface waves in a dielectric multilayer using photonic force microscopy. *J. Opt. Soc. Am. B* **2016**, *33*, 1120−1127.
(36) Martinot, P.; Koster, A.; Laval, S. Experimental observation of optical bistability by excitation of a surface plasmon wave. *IEEE J. Quantum Electron.* **1985**, *21*, 1140−1143.
(37) Lee, K.-S.; Lee, T.-S.; Kim, W.-M.; Cho, S.; Lee, S. Pump-probe optical switching in prism-coupled Au:SiO_2 nanocomposite waveguide film. *Appl. Phys. Lett.* **2007**, *91*, 141905.
(38) Chai, Z.; Hu, X.; Wang, F.; Niu, X.; Xie, J.; Gong, Q. Ultrafast all-optical switching. *Adv. Opt. Mater.* **2017**, *5*, 1600665.
(39) Novikov, I. A.; Kiryanov, M. A.; Nurgalieva, P. K.; Frolov, A. Y.; Popov, V. V.; Dolgova, T. V.; Fedyanin, A. A. Ultrafast magneto-optics in nickel magnetoplasmonic crystals. *Nano Lett.* **2020**, *20*, 8615−8619.
(40) Baida, F. I.; Bernal, M.-P. Correcting the formalism governing Bloch Surface Waves excited by 3D Gaussian beams. *Commun. Phys.* **2020**, *3*, 86.
(41) Akhmanov, S. A.; Sukhorukov, A. P.; Khokhlov, R. V. Self-focusing and diffraction of light in a nonlinear medium. *Sov. Phys. Usp.* **1968**, *10*, 609−636.
(42) Kuriakose, T.; Renversez, G.; Nazabal, V.; Elsawy, M. M. R.; Coulon, N.; Němec, P.; Chauvet, M. Nonlinear self-confined plasmonic beams: experimental proof. *ACS Photonics* **2020**, *7*, 2562−2570.
(43) Angelini, A. Resonant evanescent complex fields on dielectric multilayers. *Opt. Lett.* **2015**, *40*, 5746−5749.
(44) Angelini, A.; Lamberti, A.; Ricciardi, S.; Frascella, F.; Munzert, P.; De Leo, N.; Descrovi, E. In-plane 2D focusing of surface waves by ultrathin refractive structures. *Opt. Lett.* **2014**, *39*, 6391−6394.
(45) Angelini, A.; Barakat, E.; Munzert, P.; Boarino, L.; De Leo, N.; Enrico, E.; Giorgis, F.; Herzig, H. P.; Pirri, C. F.; Descrovi, E. Focusing and extraction of light mediated by Bloch surface waves. *Sci. Rep.* **2015**, *4*, 5428.
(46) Yu, L.; Barakat, E.; Sfez, T.; Hvozdara, L.; Di Francesco, J.; Herzig, H. P. Manipulating Bloch surface waves in 2D: a platform concept-based flat lens. *Light Sci. Appl.* **2014**, *3*, e124.
(47) Augenstein, Y.; Vetter, A.; Lahijani, B. V.; Herzig, H. P.; Rockstuhl, C.; Kim, M.-S. Inverse photonic design of functional elements that focus Bloch surface waves. *Light Sci. Appl.* **2018**, *7*, 104.

https://doi.org/10.1021/acsphotonics.1c01402
ACS Photonics 2022, 9, 211−216